Engineering Solid Mechanics 9 (2021) 123-136

Contents lists available at GrowingScience

Engineering Solid Mechanics

homepage: www.GrowingScience.com/esm

# Effect of non-linear leaflet material properties on aortic valve dynamics - A coupled fluid-structure approach

**Armin Amindari[a*], Kadir Kırkköprü[a], İrfan levent Saltık[b] and Emin Sünbüloğlu[a]**

[a]*Istanbul Technical University, Faculty of Mechanical Engineering, Turkey*
[b]*Istanbul University, Cerrahpasa Faculty of Medicine, Turkey*

**ARTICLE INFO**

*Article history*:
Received 10 October2020
Accepted 17 December 2020
Available online
17 December 2020

*Keywords*:
*Aortic Valve Leaflets*
*Valve Dynamics*
*Fluid-Structure Interaction*
*Non-Linear Material Properties*

**ABSTRACT**

Due to complex structure of aortic valve (AV) leaflets and its strong interaction with the blood flow field, realistic and accurate modeling of the valve deformations comes with many challenges. In this study, we aimed to investigate the effect of AV material properties on the valve deformations, by implementing different non-linear properties of the AV leaflets in three different material models. In the computations, we captured the dynamics between the leaflet deformations and blood flow field variations by using an iterative implicit fluid-structure interaction (FSI) approach. By comparison of the FSI simulation results of these three models, the effects of hyperelasticity and anisotropy on the valve deformations have been studied in detail. The simulation results reveal the fact that the material characteristics strongly affect the deformation characteristics of the leaflets in the systolic phase. The material anisotropy stabilizes the leaflet movements during the systolic phase, which helps decreasing the flutters of the leaflets during the peak jet blood flow. Similarly, it has been observed that the hyperelastic behavior yields an increase in the valve opening area during systolic phase which prevents the risk of excessive work of the heart due to high pressure difference. Furthermore, simulation results indicate that the stress levels in hyperelastic model are much lower, compared to the stress levels in linear elastic one. This suggests that the non-linear material character of the leaflets decreases the risk of calcification.

© 2021 Growing Science Ltd. All rights reserved.

## 1. Introduction

The heart pumps the oxygenated blood to the whole body through the aortic valve (AV) which lies at the junction with the left ventricle and the aorta. The AV is normally comprised of three luminal leaflets. However, in some cases it is found that the AV has congenitally only two cusps. The cusps are anatomically restricted to open in one direction to ensure the unidirectional flow of the blood flow through the aortic valve. Consequently, the efficient transport of blood cells to the whole body relies on the proper function of three cusps. Any structural abnormality of the leaflets can lead to serious diseases associated with high mortality and morbidity unless treated properly. The narrowing of the AV opening during systole phase which is the most prevalent of all valve disorders is called aortic stenosis. Aortic stenosis may be caused by a congenital heart defect or by other conditions such as accumulation of calcium deposits on the AV leaflets. Aortic valve regurgitation is another serious leaflet dysfunction, which is associated by diastolic backflow of the blood from aorta to the left ventricle. The severity of

* Corresponding author.
E-mail addresses: amindari@itu.edu.tr (A. Amindari)

© 2021 Growing Science Ltd. All rights reserved.
doi: 10.5267/j.esm.2021.1.001

AV diseases is evaluated by several test standards. Depending on the severity of disease different treatment plans can be adopted by physicians (Ho, 2009; Petrou & Shah, 2018; Lindman et al., 2016). Since AV disease is a structural dysfunction, it can only be managed using mechanical treatments. For patients with severe AV diseases, aortic valve replacement is the most effective treatment standard, in which the AV is replaced with a mechanical or biological one. Through the different options for the valve replacement operations, the transcatheter aortic valve replacement (TAVR) is known to be less invasive and traumatic. However, the valve which is used for the replacement should offer proper hemodynamic performance and lifelong durability quality. Disturbed hemodynamics can lead to serious conditions like hemolysis which is associated with high shear stresses. The valve tissue should guarantee a perfect physiological hemodynamics and also be safe for blood-material reactivity. By this means, efforts to create stronger durable valves using tissue engineering are rising between researchers (Miller et al., 2012; Maxfield et al., 2014; Hinderer et al., 2014). Although bold steps have been made toward creating functional valve tissue, the developed materials still need better biocompatibility and bi-functionality. The successful development of the artificial valve tissue solely relies on accurate and detailed investigation of natural human valve structure. However, realistic and accurate modeling of the valve deformations using numerical models comes with many challenges.

There are numerous studies that have been focused only on the valve hemodynamics and neglected the non-linear behavior of aortic valve material for simplicity (Luraghi et al., 2017; Soares et al., 2014; Marom et al., 2013; Piatti et al., 2015). All these studies contributed substantially to our understanding of the AV dynamics. However, it has been known that the AV material response during the deformation of the valve from the initial position to a deformed shaped is non-linear. For an accurate and realistic simulation of the valve deformation the nonlinear properties of the valve must be implemented in detail to the material model.

Studies concerning the non-linear behavior of the AV have revealed important insights about AV dynamics (Sturla et al., 2016; Grande et al., 2000; Li et al., 2010). Koch et al. (2001) have studied the nonlinear properties of the AV using different material models. By comparing these material models, impact of material properties on the valve dynamics was studied in detail. Although these studies have shown imported aspects of valve dynamics, they had an important limitation due to ignoring the fluid dynamics and relying only on the structural mechanics and finite element analysis. The blood flow and viscous stresses exerts pressure on the leaflets and the response of the aortic valve to this pressure variation alters the hemodynamics of the blood flow around the AV strongly. Thus, for accurate investigation of the relation between nonlinear AV properties and the deformations of the leaflets, the blood flow and the structure fields must be modeled simultaneously in a coupled approach. In the recent years, investigating the non-linear properties of the AV and its interaction with the blood flow is in focus interest of researchers. However, there are still many unknowns about the non-linear behavior of the leaflet's material. These unknowns have to be revealed and studied accurately for developing an optimum functional aortic valve tissue that can be safely replaced with a diseased AV.

In the current study, non-linear characteristics of the aortic valve leaflets have been investigated using a coupled FSI approach. Models have been created with 3 different material models. The first model has been developed using an isotropic linear elastic material model assuming a linear relation between strain and stress. Furthermore, for the second model, an isotropic hyper elastic material model has been adopted to characterize the nonlinear behavior of the aortic valve leaflets. Finally, for the third model, the anisotropic characteristics of the leaflet material properties have been characterized using a linear transversely orthotropic material model.

## 2. Computational Model and Methods

### *2.1 Geometry and discretization*

The unpressurized 3D geometry of the AV leaflet structure and blood flow volume is created using 5 design parameters as shown in Fig. 1a. The values of each design parameter used for this study is given

in Table 1. The valve thickness is assumed as constant value of 0.6 mm (Stradins et al. 2004). First order tetrahedral elements have been used for discretizing the solution filed. Mesh convergence analysis has been performed to capture the element size sensitivity. It has been observed that by using minimum number of 12,000 for leaflet structure field and 240,000 elements for the blood flow field the numerical results will indicate satisfactory stability. To avoid shear locking in leaflets 3 elements with the length of 0.2 mm has been fitted through the thickness of the AV. To capture the flow boundary layer near the leaflets more accurately, finer mesh density has been used in the leaflet and sinus area in the blood flow discretization field. The discretized solution field both for AV leaflet structure and blood flow zones is shown in Fig. 1b.

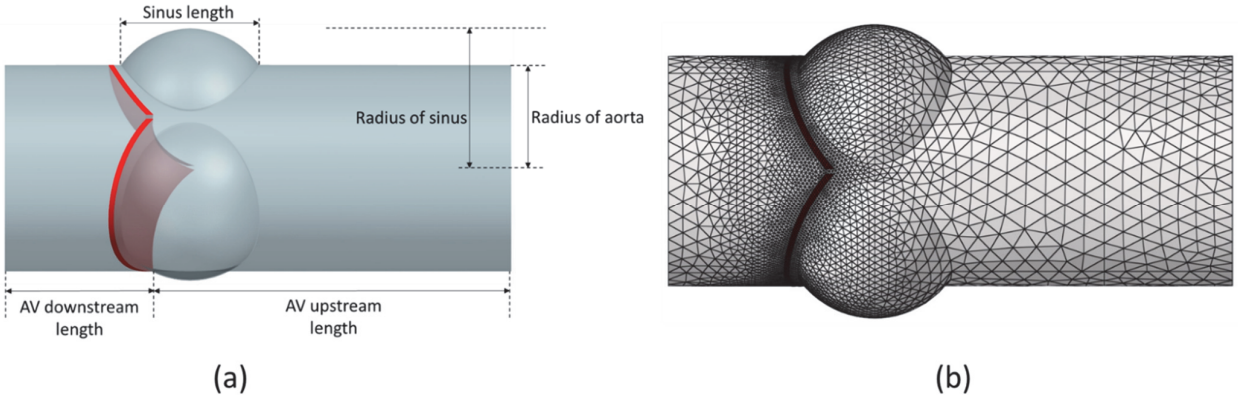


**Fig. 1.** a) Geometry design of the AV solution field using the modeling design parameters b) Discretization of solution field by tetrahedral elements

**Table 1.** Dimensions of de sign parameters used in modeling the AV

| | ra | rs | sl | usl | dsl |
|---|---|---|---|---|---|
| Dimension (mm) | 10 | 13.17 | 12.12 | 13 | 31 |

ra: radius of aorta, rs: radius of sinus, sl: sinus length, dsl: downstream length, usl: upstream length

*2.2 The Leaflet structural field*

The AV leaflets are complex thin structures which are made up of valve interstitial cells (VIC), extracellular matrix (ECM) and endothelial cells on arterial and ventricular surfaces. The ECM is an extracellular network of collagen, elastin, Glycosaminoglycans. Various compositions of these molecules through the thickness of the leaflets, forms three distinctive layers. These layers are namely: the fibrosa in the aortic side, the ventricularis in the ventricle side and the spongiosa between fibrosa and ventricularis layers as shown in Fig. 2.

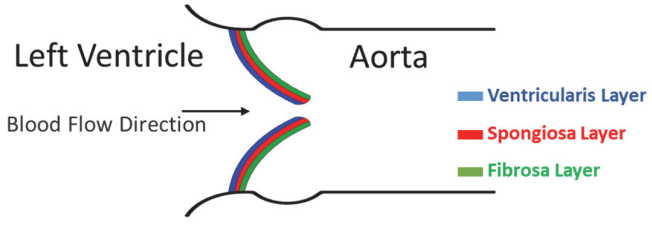


**Fig. 2.** Three distinctive layers of the aortic valve; Fibrosa, Spongiosa and Ventricularis layers

Each layer contributes to ensure optimal hemodynamic and mechanical environment without any abnormal hemodynamic disturbance. The fibrosa is dominantly composed of collagen fibers oriented in circumferential direction. Collagen, which is the most abundant structural protein in mammals, provides high tensile strength for the fibrosa layer. The circumferential orientation of the collagen fibers makes

fibrosa 4-6 times stiffer in the circumferential direction than other directions. The ventricularis layer, on the other hand consists of organized networks of elastin fibers. Elastin which is a highly elastic protein allows the elastic recoil of the leaflets, as well as maintaining the shape of collagen fibers. The spongiosa majorly consists of glycosaminoglycans with high amount of water which has not a significant effect on the rigidity behavior of the aortic valve (Hinton & Yutzey, 2011; Yutzey et al., 2014).

The deformation of the aortic valve tissue under blood flow forces is highly non-linear due to these distinctive layers. In this study three different material models have been developed to investigate the effect of leaflets non-linearity on the valve deformations. These material models are; isotropic linear elastic material model, isotropic hyper elastic material model and finally anisotropic material model. To derive these mathematical models, uniaxial tension tests must be performed on the real leaflet tissue. In this study the uniaxial test data presented by Stardins et al. (2004) has been used for deriving the materials mathematical models. The stress-strain curves for radial and circumferential direction for leaflet materials have been shown in Fig. 3.

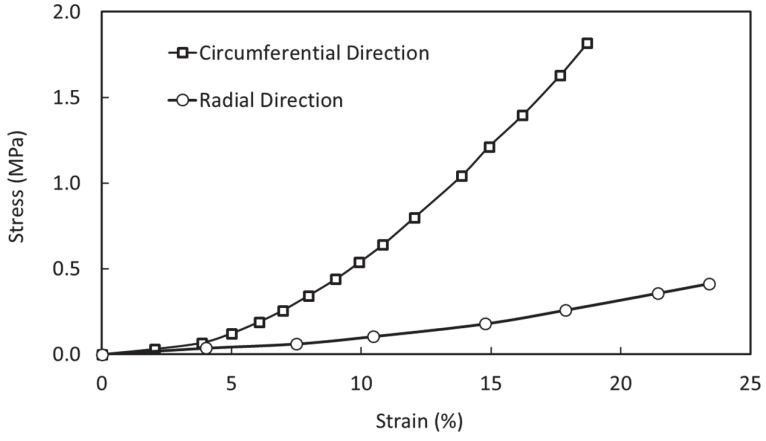


**Fig. 3.** Stress-strain curves for aortic valve tissue in radial and circumferential directions

*2.2.1 Case 1: Linear Elastic Isotropic Model (LEI Model)*

For Linear Elastic Isotropic **(**LEI) model the anisotropic behavior of the AV leaflets due to existence of collagen fibers is excluded from calculations and it was assumed that the elastic properties remain constant in every direction inside the leaflet material. Additionally, it was assumed that there is a linear relation between the stress and strain. The constitutive equation for LEI material can be expressed as Hooke's Law as shown in Eq. (1).

$$\varepsilon_{ij} = \frac{1}{E}\,(\sigma_{ij} - \nu(\sigma_{kk}\delta_{ij} - \sigma_{ij})). \tag{1}$$

Two independent elastic constants which are needed to determine the mechanical behavior of LEI material model are the Young's modulus (E) and the Poisson's ratio ($\nu$). The average strain of leaflets during a cardiac cycle can be estimated as 10 % (Thubrikar et al., 1980). Thus, in this study the Young's modulus for the LEI material is approximated as the calculated secant modulus of strain-stress curve in radial direction for 10 % strain. The calculated secant modulus value is 1 MPa and is defined as modulus of elasticity of leaflet materials for LEI model to ensure the proportional relation between the stress and strain. Furthermore, the Poisson's ratio is set to 0.49 for ensuring the incompressibility behavior of the AV leaflet material. The LEI model (Case 1) resembles the case as if there were no collagen fibers inside the AV leaflets and also as if there was a linear relation between the stress and strain.

*2.2.2 Case 2: Hyper elastic Isotropic Model (HEI Model)*

The nonlinear relation between stress and strain has been implemented to the hyper elastic Isotropic (HEI) material model by adopting a hyper elastic constitutive material model. However, in this case also the effect of collagen fibers orientation in the circumferential directions of the leaflets has been excluded and it was assumed that the elastic properties remain the same in all directions. 1st order Ogden hyper elastic model has been used to fit the stress strain curve in the radial direction for the material model ( $\mu_1$ = 39.73 Mpa and $\alpha_1$=12.24). The strain energy function for the first order Ogden hyper elastic model can be expressed as Eq. (2).

$$W(\lambda_1, \lambda_2, \lambda_3) = \frac{\mu}{\alpha_1}(\lambda_1{}^{\alpha_1} + \lambda_2{}^{\alpha_1} + \lambda_3{}^{\alpha_1} - 3), \tag{2}$$

where $\lambda_1$, $\lambda_2$ and $\lambda_3$ are the principal stretches and the $\mu$ and $\alpha_1$ are material constants.

The Ogden material model created by fitting the experimental stress strain-curve is validated by performing quasi static analysis. For the validation study, sample geometry has been created with the dimensions similar to the dimensions of specimen used in experimental uniaxial tests. By applying a pressure load profile on one end of the geometry the total deformation of the specimen has been calculated. The results of the numerical calculations and the experimental results are compared in Fig. 4. It can be observed that the Ogden hyper elastic model created for HEI model has good agreement with the experimental results.

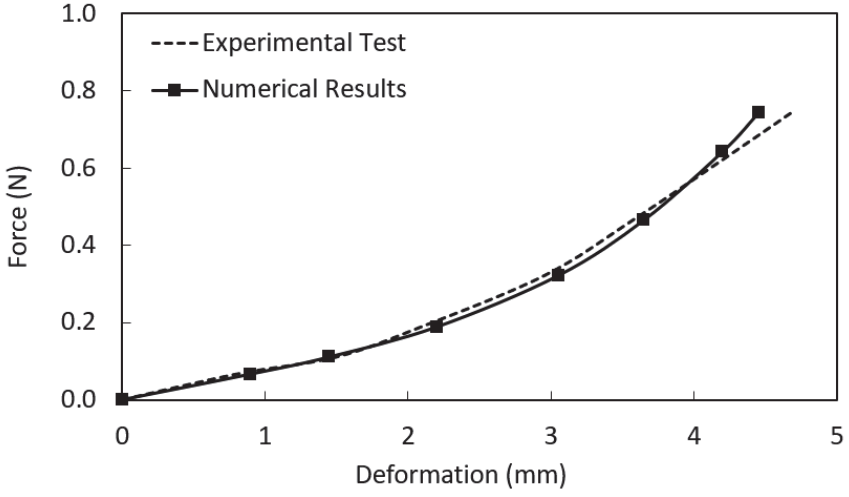


**Fig. 4.** Comparison of the experimental uniaxial test results with the numerical results of the fitted Ogden material model

*2.2.3 Case 3: Linear Elastic Anisotropic Model (LEA Model)*

Anisotropic behavior of the AV leaflets is implemented in the third case (LEA Model) using a transversely isotropic material model. Due to orientation of the collagen fibers in circumferential direction the rigidity of leaflets in this direction is much higher than other directions. The elastic properties of the leaflets in axial and radial directions can be assumed equal. To derive the LEA model, stress-strain curves in radial and circumferential directions (Fig. 3) are used separately.

The generalized Hook's law for an anisotropic material which defines the relation among all the stress and strain tensor material can be written as Eq. (3).

$$\sigma_{ij} = C_{ijkl}\,\varepsilon_{kl}. \tag{3}$$

Here, $\sigma_{ij}$, $\varepsilon_{kl}$ and $C_{ijkl}$ are the components of the stress, infinitesimal strain and fourth-order stiffness tensors respectively. The elasticity tensor $C_{ijkl}$ for any material has 81 members. However, due to symmetric nature of the stress, strain and elastic strain tensors, the independent elastic constants of the $C_{ijkl}$ tensor for a fully anisotropic material reduces to 21. For the case of orthotropic materials with 3 mutually orthogonal planes of material symmetry the number of independent elastic constants reduces to 9. The compliance matrix for an orthotropic material can be written as:

$$S = {C_{ijkl}}^{-1} = \begin{bmatrix} \frac{1}{E_1} & -\frac{\nu_{21}}{E_2} & -\frac{\nu_{31}}{E_3} & 0 & 0 & 0 \\ -\frac{\nu_{12}}{E_1} & \frac{1}{E_2} & -\frac{\nu_{32}}{E_3} & 0 & 0 & 0 \\ -\frac{\nu_{13}}{E_1} & -\frac{\nu_{23}}{E_2} & \frac{1}{E_3} & 0 & 0 & 0 \\ 0 & 0 & 0 & \frac{1}{G_{23}} & 0 & 0 \\ 0 & 0 & 0 & 0 & \frac{1}{G_{13}} & 0 \\ 0 & 0 & 0 & 0 & 0 & \frac{1}{G_{12}} \end{bmatrix}. \quad (4)$$

Here circumferential, axial and radial directions are denoted by numbers 1, 2 and 3 respectively. $E_i$ is the modulus of elasticity in $i$ direction. Similarly, $\nu_{ij}$ and $G_{ij}$ are Poisson's ratio and shear modulus in $ij$ plane respectively. Furthermore, it is known that the collagen fibers of the leaflets are mainly oriented only in circumferential direction. Thus, only a single material direction in circumferential direction exists, whose mechanical properties in the orthogonal plane to this direction can be assumed as isotropic. As a result, mechanical properties of the leaflets at every point on the plane perpendicular to circumferential direction are same in every direction. Consequently, the valve leaflets can be sub categorized as transversely isotropic material. Using this assumption, the number of independent elastic constants reduces to only five independent elastic constants. Due to existence of plane of isotropy in the plane orthogonal to circumferential direction one can easily conclude that $E_2 = E_3$. The $E_1$ is estimated by calculating the secant modulus of the stress-strain curve in circumferential direction at the strain level of 10% which is equal to 5.48 MPa. Similarly, $E_2, E_3$ are estimated by calculating the secant modulus of the stress strain curve in the radial direction which is equal to 1 MPa. Similarley the poission's ratio for $\nu_{12}$ and $\nu_{23}$ is defined as 0.45 to approximate the incompressbility in these planes. Using this transversly isotropic model the anistropy behaviour of the AV leaflets is implememented in LEA model. For all the three material models the density of the structures are defined as 1060 kg/m$^3$ to avoid bouyancy effects.

*2.3 The blood flow field*

Blood is composed of red blood cells, white blood cells and platelets which are suspended in plasma. The viscosity of the blood decreases with the shear rate and is categorized as a shear-thinning fluid. However, in large blood vessels like the aorta where the shear rate is above 100 s$^{-1}$ the blood can be assumed as a Newtonian fluid (Kudenatti et al. 2012). In this study, the dynamic viscosity of the blood fluid is defined as a constant value of 3.785 × 10$^{-3}$ Pa. s for the FSI simulations (Kudenatti et al. 2012).

The peak velocities inside the blood flow domain is much lower than the speed of sound wave and only small density variations can occur inside the flow domain. As a consequence, the blood flow over the AV is assumed incompressible. Thus, for the simulations, the density of the blood fluid is defined as a constant value of 1060 Kg/m$^3$.

The peak Reynolds number regarding the aortic blood flow, which is calculated based on the AV diameter and flow properties is around 5000. Due to pulsatile nature of the flow and the moving complex

flow domain, turbulent flow regions may form downstream of the aortic valve. In this paper, the turbulent characteristics of the blood flow is modeled using k-e realizable model, due to strength of this model in predicting the spread rate of round jets more accurately and also having better performance for flows involving rotation, separation and recirculation. The inlet turbulence intensity has been defined as 1.5 % for employing the k-e realizable model. Moreover, the viscosity affected region between the endothelium and the turbulent flow region has been bridged using standard wall function.

The governing equations of the blood flow through the aortic valve consist of conservation of mass and the momentum equations. Respectively, by assuming Newtonian fluid and incompressible flow, the conservation of linear momentum equations may be expressed as follows.

$$\nabla . \left(\vec{U}\right) = 0 \tag{5}$$

$$\frac{\partial \vec{U}}{\partial t} + \vec{U}\left(\nabla . \vec{U}\right) = -\frac{\overrightarrow{\nabla p}}{\rho} + \nabla . (\upsilon \nabla \vec{U}) \tag{6}$$

The flow has been assumed isothermal. Thus, the energy equation is not included for the simulations. During systolic phase, an electrical impulse triggers the left ventricle muscles leading to rapid contraction of the left ventricle tissue. This contraction applies pressure on the blood inside the ventricle forcing it to leave the heart through the aortic valve. For an accurate and realistic simulation of the blood flow through the aortic valve the upstream aortic valve pressure profile must applied as a boundary condition for the blood flow. The pressure applied on the blood inside the ventricle can be measured by catheter angiography(Nishimura & Carabello, 2012). In this study the transvalvular pressure profile during the systolic phase, which is shown in Fig. 5 has been applied as pressure inlet boundary condition for the FSI simulations. The time between 0 s and 0.3 s corresponds to the systolic phase in the Fig. 5. During the systolic the blood in the ventricle is passed through the aortic valve and enters the aorta.

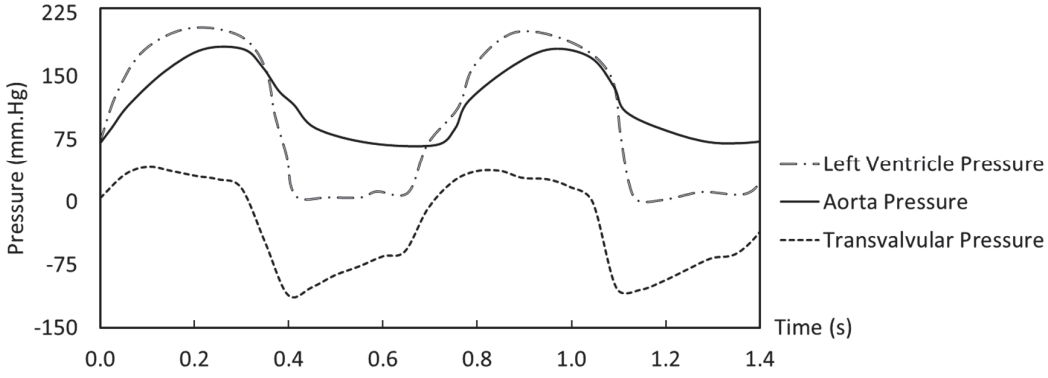


**Fig. 5.** Left ventricle, aorta and transvalvular pressure profile used as boundary condition for FSI simulations (Bonow et al. 2011)

The Navier Stokes and turbulent equations are solved using the commercial CFD solver ANSYS™ FLUENT™ (version 19.0) which utilizes the finite volume methods for solving the flow equations.

*2.4 Fluid- Structure Interaction (FSI) Coupling*

As discussed earlier the blood flow and the leaflet structure are in strong interaction with each other. The blood flow exerts hydrodynamic pressure on the leaflets and leaflets are deformed elastically under these pressure variations between the downstream and upstream of the aortic valve. Thus solving only AV structure field separately will neglect this interaction and may lead to incorrect analysis. In this study the structure and the flow fields are coupled together using an iterative implicit method. This iterative method will ensure that the interaction between the flow fields and structures fields will be captured accurately. Using this method in each time step the flow and structure fields are solved simultaneously

with two separate CFD and FEM solvers. At the end of each time step the information regarding the pressure field of the blood flow and the deformation of the leaflets are shared between solvers using an iterative method. More detailed information about the iterative implicit FSI approach which is used in this study is given by (Amindari et al. 2017).

## 3. Results

### *3.1 AV leaflet deformation*

The deformation of AV leaflets under blood flow is calculated using FSI simulations. Fig. 6 shows the deformation of AV leaflets for LEI, HEI and LEA models for different time intervals. It can be observed that the maximum deformation of the AV leaflets occurs at the peak blood velocity. Similarly, the deformation plots show that the HEI model undergoes higher deformation with respect to other two AV models. For accurate comparison of the AV models, quantitative models are discussed in next parts of this study.

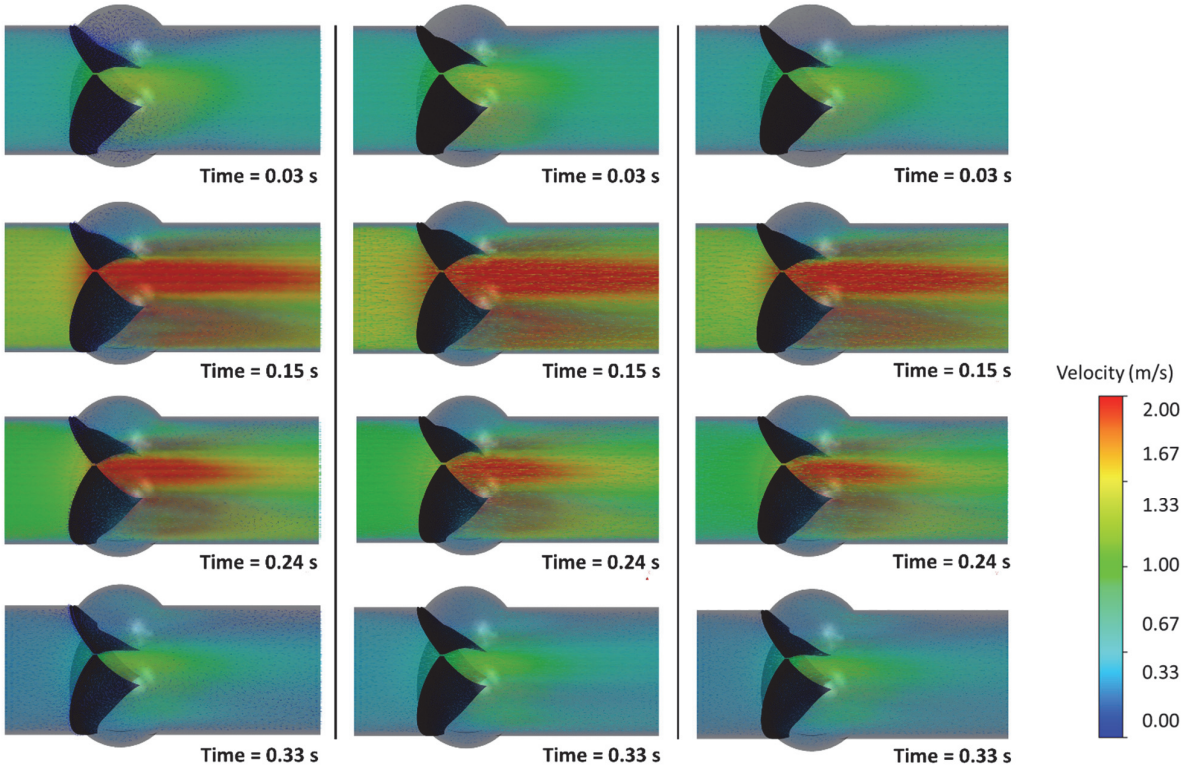


**Fig. 6.** FSI deformation results for a) Linear elastic isotropic model b) Hyperelastic isotropic model c) Linear elastic anisotropic model

### *3.2 Geometrical Orifice Area*

To investigate the deformation behavior of the AV leaflets interacting with the blood flow more accurately, time dependent geometrical orifice area (GOA) can be calculated quantitatively. In this study, the GOA is calculated by processing the images created by post processing the FSI results. In this method the pixels inside the valve orifice area is counted using a color threshold algorithm. Accordingly, the orifice area is calculated by multiplying the area of a single pixel by total number of counted pixels. The time dependent GOA for the three different valve models, including LEI, HEI and LEA AV models is shown in Fig. 7.

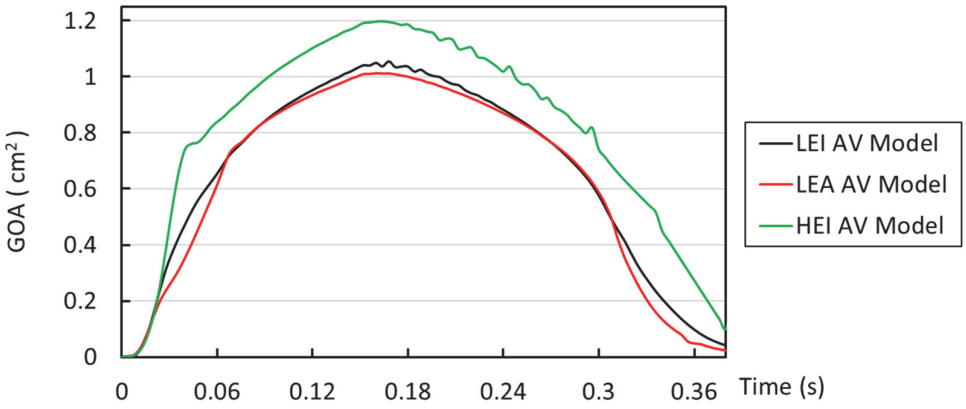


**Fig. 7.** Time dependent GOA profiles for LEI, HEI and LEA AV models

The GOA profiles show that in all of the three control models, the valve start to open rapidly in the beginning of systole phase. Following this phase, the valve remains open steadily. While, in the last part of systole the valve closes rapidly. On the other hand, by investigation of the GOA profiles in more detail, it can be observed that after the opening phase, when the valve starts to close, significant oscillations occur in LEI and HEI models. These oscillations can be related to the flutters of the leaflets under blood pressure variations between downstream and upstream of the leaflets. However, in the LEA model these oscillations are not significant. These phenomena demonstrate the effects of collagen fibers in the stability behavior of the AV leaflets. The collagen fibers which are oriented in circumferential direction, stabilizes the leaflets during the closing phase of valve and minimizes the oscillations of leaflets.

Moreover, by comparing the maximum calculated GOA for the AV models, it can be observed that added stiffness in circumferential direction by introducing the collagen fibers, reduces the maximum GOA. However, this reduction is negligibly small. On the other hand, maximum calculated GOA during the systolic phase for the HEI AV model is higher than those of other two models. The reason for the difference in GOA level for this model is that, the strain levels during a cardiac cycle are smaller than %15 in most sections of the leaflets. Due to small slope of the strain-stress curve of AV leaflet material for strains below the %15 level, the AV leaflets behave more flexibly in the HEI AV model. Thus, it can be concluded that the hyper elasticity character of the HEI model helps AV leaflets open more easily which in turn leads to smaller blood pressure drops and better functionality.

Another important conclusion that can be made from Fig. 11 is that the in LEA AV model, leaflets tend to close much faster than other two models. The introduced rigidity in circumferential direction in orthotropic model helps the leaflets retain their initial position in the diastolic phase faster. However, in the linear elastic and hyper elastic models the leaflets remain slightly open even after the systolic phase. This may lead to severe health problems such as regurgitation disease which is caused by the backflow of the blood from the aorta to the left ventricle.

### *3.2 Mechanical Stress*

Mechanical stress has been known as an important factor for calcification of leaflets which leads to serious diseases such as severe aortic valve stenosis. The calcification on the leaflets is developed by local degeneration of valve tissue due to high mechanical stresses. Following the initiation of calcification, the calcified patterns may continue along other parts of the valve with lower mechanical stresses, (Morvan et al., 2019). In this study, the mechanical stresses on the leaflets have been quantified and compared to each other by calculating the maximum principal stress values. The contours of maximum principal stress during different time intervals of the systolic phase have been plotted in the Fig. 8 for the three different AV models.

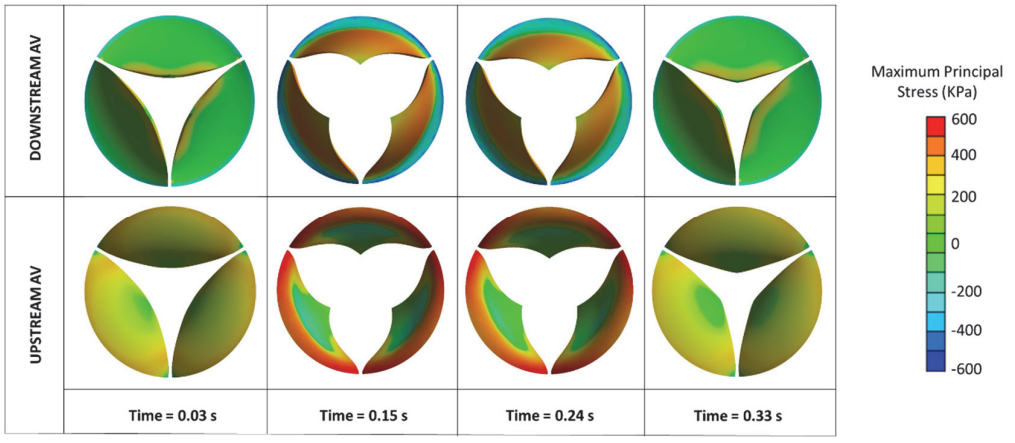


(a) LEI AV Model

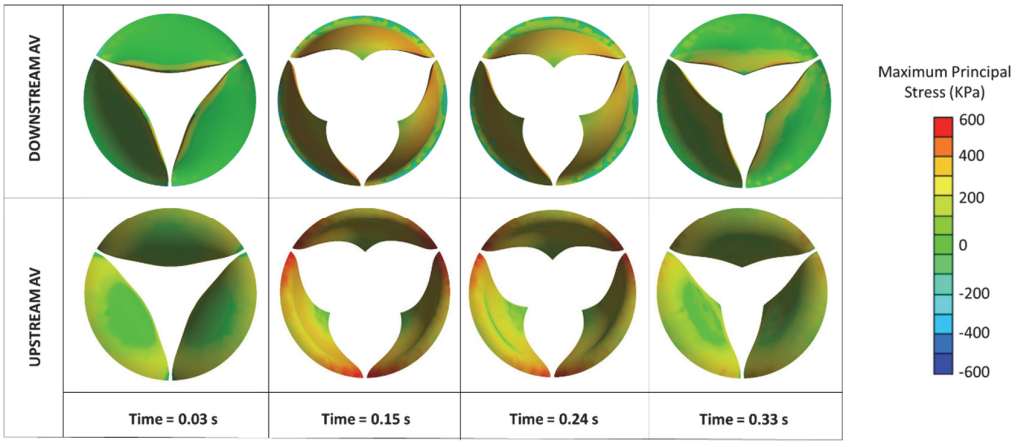


(b) HEI AV Model

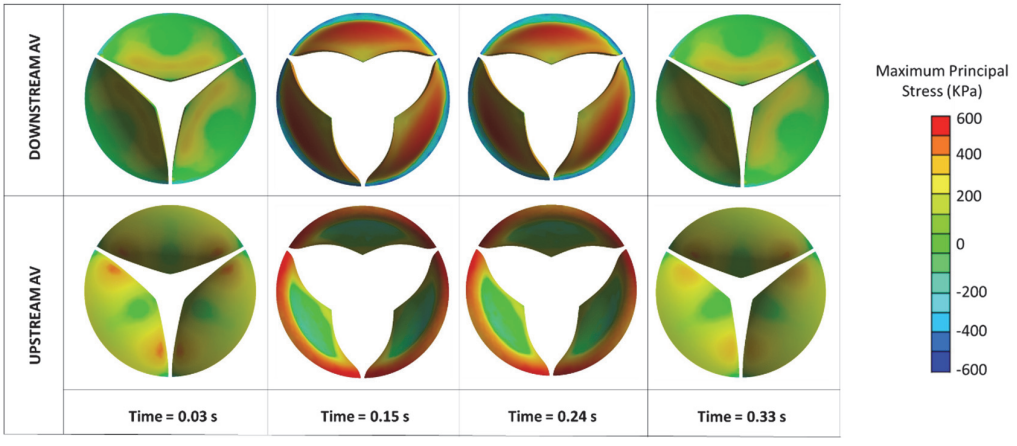


(c) LEA AV Model

**Fig. 8.** Max principal stress for a) LEI AV Model, b) HEI AV Model and c) LEA AV Model

In order to compare the stress levels more accurately, three control points have been defined on different sections of the AV leaflets as shown in Fig. 9a. Point 1 refers to the free edges of the leaflets. Similarly, point 2 refers to coaptation area and point 3 refers to attachment points of the leaflets to the aorta (Fig. 9b).

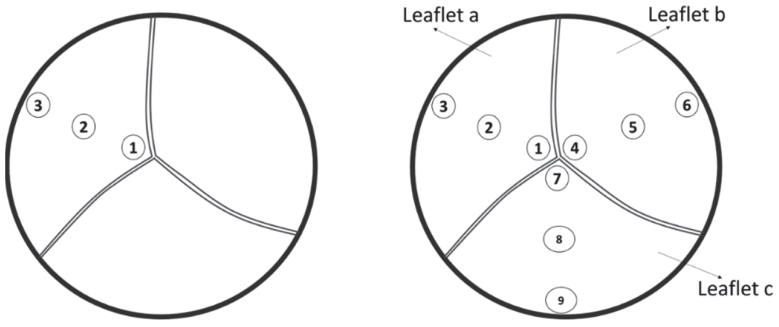


(a) (b)

**Fig. 9.** a) Control points on one cusp of AV to compare the stress level in different sections of the leaflets b) Control points on 3 cusps to compare the symmetry behaviour in the leaflets

The time dependent stress profiles for these points are plotted and compared in Figs. 10a, 10b and 10c. These results show that the mechanical stress levels for HEI model is much lower than the LEI and LEA models. Thus, it can be concluded that the hyper elastic character of AV material reduces the stress levels on the AV leaflets; suggesting that the AV with hyper elastic behavior has the lowest risk of calcification and aortic stenosis. On the other hand, by comparison of the stress levels on different sections of the leaflets (Fig. 10d) it can be observed that the stress level in free edges of leaflets (Point 1) is almost near zero and these locations can be considered as free stress zones. Using this information, it can be concluded the calcification patterns on the leaflets first initiate on the coaptation areas and leaflets edges and continue along free edges which are supposed to lower mechanical stress levels.

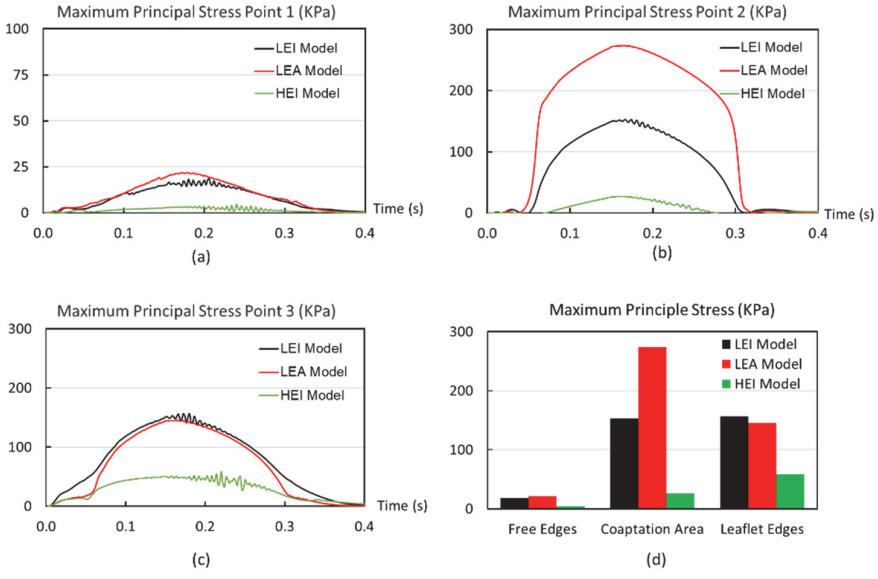


**Fig. 10.** Time dependent maximum principal stress profile for LEA, LEA and HEL models at a) Point 1 b) Point 2 c) Point 3 d) Comparison of the stress levels in different sections of the AV

In order to investigate the axisymmetric behavior of the leaflets, 9 points are defined on the AV model as shown in Fig. 9b. Points 1, 4 and 7 refer to free edge of each leaflet. Points 2, 5 and 8 are located in the coaptation sections. Similarly points 3, 6 and 9 are representing the leaflet edges of each leaflet of AV. The maximum value for maximum principal stress during a systolic phase of cardiac cycle has been calculated for each of these points (see Fig. 11). Although the leaflets geometries are axisymmetric, the investigation of stress levels on the similar locations of each leaflet of aortic valve shows that the stress distribution on the leaflet is not perfectly axisymmetric. This behavior can be related to existence of asymmetric vortexes behind the leaflets which are strongly in interaction with leaflets. Furthermore, in

natural human AV where the leaflets shapes are not exactly same as each other, the mechanical stress on the leaflets is predicted to be distributed more asymmetrically.

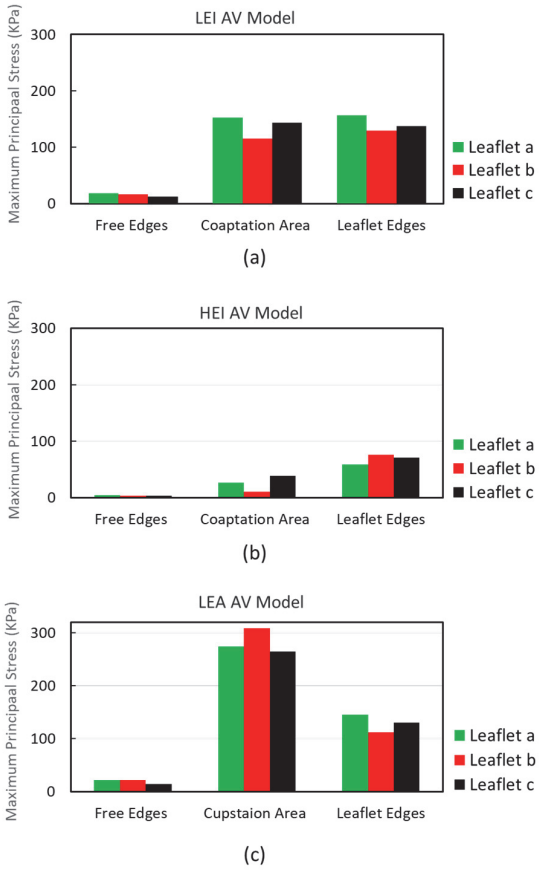


**Fig. 11.** Maximum principle stress on different areas of the leaflets a) LEI AV model, b) HEI AV Model and c) LEA AV Model

## 4. Conclusion

Currently, research on AV dynamics is mostly focused on the development of proper replaceable AV tissue. However, development of ideal AV with proper hemodynamic function relies on accurate and complete investigation of AV natural tissue and our enough understanding of its nonlinear behavior.

In this study, we aimed to study the effect of nonlinear properties of the AV tissue on the AV deformations using three-dimensional fluid-structure interaction (FSI) models. The simulation results clearly show that the blood flow pressure variations dominate the valve deformations and dynamics. Using this FSI approach, we investigated the material anisotropy and hyperelasticity behavior of the AV tissue and its effect on valve dynamics in detail.

For an accurate and quantitative comparison of the performance of each control model we derived the time dependent GOA profile for each control model by processing the images created by simulation results. The GOA profiles clearly revealed the fact that the material nonlinear properties have a dominant effect on the AV dynamics. By comparison of the GOA profile of three models, we observed that the collagen fiber orientation in the circumferential direction has a noticeable effect on stabilizing the valve deformations, which leads to lower oscillations and less flutters of the leaflets. Similar results have been also reported by De Hart et al. (2004) by qualitative comparison of valve AV images. However, we were able to prove this behavior using quantified GOA plots. Furthermore, the GOA profiles also revealed that the closing phase of the AV leaflets is also affected strongly by the collagen fibers. By this means, the

role of the added rigidity in circumferential direction for helping the leaflets to retain their closed shape became more apparent (Hammer et al., 2014; Loerakker et al., 2013).

In order to evaluate the calcification risk, we compared the mechanical stress levels on different parts of the leaflets. While the calculated mechanical stress in the free edges area near zero, we noticed high stress values in coaptation area and leaflet edges regions. These results suggest that the calcification patterns on the leaflets first initiate from the coaptation and leaflet edges surfaces. The MRI images captured from calcified aortic valve leaflets in a previous study (Ovcharenko et al. 2017) confirm these results. The maximum principal stress for LEI, LEA and HEI models in the coaptation area are calculated as 152 kPa, 263 kPa and 26 kPa, respectively. The comparison of stress levels shows that hyperelastic AV is prone to slightly lower mechanical stresses distribution on the leaflets. Using these results, one may conclude that the hyperelasticty character of the AV reduces the risk of calcification.

For future work a patient specific FSI model can be created using non uniform leaflet thickness and valve dimensions, which can be measured by MRI images. Furthermore, the non-Newtonian blood model can also be made by testing the blood sample of the same patient. The pressure inlet boundary condition can be obtained by performing catheter angiography on the patient to derive the pressure profile in upstream and downstream of the AV.

In this work, we focused on the effect of the material nonlinearity on the valve deformations and dynamics. Nevertheless, the material properties and valve dynamics also alter the hemodynamics and flow properties strongly. We are currently working to characterize this influence by studying the AV flow field models in detail.

## References


Amindari, A., Saltik, L., Kirkkopru, K., Yacoub, M., & Yalcin, H. C. (2017). Assessment of calcified aortic valve leaflet deformations and blood flow dynamics using fluid-structure interaction modeling. *Informatics in Medicine Unlocked*, *9*, 191-199.

Bonow, R. O., Mann, D. L., Zipes, D. P., & Libby, P. (2011). *Braunwald's heart disease e-book: A textbook of cardiovascular medicine*. Elsevier Health Sciences.

De Hart, J., Peters, G. W. M., Schreurs, P. J. G., & Baaijens, F. P. T. (2004). Collagen fibers reduce stresses and stabilize motion of aortic valve leaflets during systole. *Journal of Biomechanics*, *37*(3), 303-311.

Elert, G. (2011). Viscosity. The Physics Hypertextbook. by Glenn Elert. *Hypertextbook. com. Retrieved*, 02-02.

Grande, K. J., Cochran, R. P., Reinhall, P. G., & Kunzelman, K. S. (2000). Mechanisms of aortic valve incompetence: finite element modeling of aortic root dilatation. *The Annals of Thoracic Surgery*, *69*(6), 1851-1857.

Hammer, P. E., Pacak, C. A., Howe, R. D., & Pedro, J. (2014). Straightening of curved pattern of collagen fibers under load controls aortic valve shape. *Journal of Biomechanics*, *47*(2), 341-346.

Hinderer, S., Seifert, J., Votteler, M., Shen, N., Rheinlaender, J., Schäffer, T. E., & Schenke-Layland, K. (2014). Engineering of a bio-functionalized hybrid off-the-shelf heart valve. *Biomaterials*, *35*(7), 2130-2139.

Hinton, R. B., & Yutzey, K. E. (2011). Heart valve structure and function in development and disease. *Annual Review of Physiology*, *73*, 29-46.

Ho, S. Y. (2009). Structure and anatomy of the aortic root. *European Journal of Echocardiography*, *10*(1), i3-i10.

Koch, T. M., Reddy, B. D., Zilla, P., & Franz, T. (2010). Aortic valve leaflet mechanical properties facilitate diastolic valve function. *Computer Methods in Biomechanics and Biomedical Engineering*, *13*(2), 225-234.

Kudenatti, R. B., Bujurke, N. M., & Pedley, T. J. (2012). Stability of two-dimensional collapsible-channel flow at high Reynolds number. *Journal of Fluid Mechanics*, *705*, 371.

Li, J., Luo, X. Y., & Kuang, Z. B. (2001). A nonlinear anisotropic model for porcine aortic heart valves. *Journal of Biomechanics*, *34*(10), 1279-1289.

Lindman, B. R., Clavel, M. A., Mathieu, P., Iung, B., Lancellotti, P., Otto, C. M., & Pibarot, P. (2016). Calcific aortic stenosis. *Nature reviews Disease primers*, *2*(1), 1-28.

Loerakker, S., Argento, G., Oomens, C. W., & Baaijens, F. P. (2013). Effects of valve geometry and tissue anisotropy on the radial stretch and coaptation area of tissue-engineered heart valves. *Journal of Biomechanics*, *46*(11), 1792-1800.

Luraghi, G., Wu, W., De Gaetano, F., Matas, J. F. R., Moggridge, G. D., Serrani, M., ... & Migliavacca, F. (2017). Evaluation of an aortic valve prosthesis: Fluid-structure interaction or structural simulation?. *Journal of Biomechanics*, *58*, 45-51.

Marom, G., Haj-Ali, R., Rosenfeld, M., Schäfers, H. J., & Raanani, E. (2013). Aortic root numeric model: Annulus diameter prediction of effective height and coaptation in post–aortic valve repair. *The Journal of Thoracic and Cardiovascular Surgery*, *145*(2), 406-411.

Maxfield, M. W., Cleary, M. A., & Breuer, C. K. (2014). Tissue-Engineering Heart Valves. In *Principles of Tissue Engineering* (pp. 813-833). Academic Press.

Miller, D. C., Blackstone, E. H., Mack, M. J., Svensson, L. G., Kodali, S. K., Kapadia, S., ... & Webb, J. G. (2012). Transcatheter (TAVR) versus surgical (AVR) aortic valve replacement: occurrence, hazard, risk factors, and consequences of neurologic events in the PARTNER trial. *The Journal of Thoracic and Cardiovascular Surgery*, *143*(4), 832-843.

Morvan, M., Arangalage, D., Franck, G., Perez, F., Cattan-Levy, L., Codogno, I., ... & Michel, J. B. (2019). Relationship of iron deposition to calcium deposition in human aortic valve leaflets. *Journal of the American College of Cardiology*, *73*(9), 1043-1054.

Nishimura, R. A., & Carabello, B. A. (2012). Hemodynamics in the cardiac catheterization laboratory of the 21st century. *Circulation*, *125*(17), 2138-2150.

Ovcharenko, E. A., Klyshnikov, K. U., Glushkova, T. V., Batranin, A. V., Rezvova, M. A., Kudryavtseva, Y. A., & Barbarash, L. S. (2017). Evaluation of a Failed Heart Valve Bioprosthesis Using Microcomputed Tomography. *Современные технологии в медицине*, *9*(3 (eng)).

Petrou, L., & Shah, B. N. (2018). Aortic valve disease. *Medicine*, *46*(11), 676-681.

Piatti, F., Sturla, F., Marom, G., Sheriff, J., Claiborne, T. E., Slepian, M. J., ... & Bluestein, D. (2015). Hemodynamic and thrombogenic analysis of a trileaflet polymeric valve using a fluid–structure interaction approach. *Journal of Biomechanics*, *48*(13), 3641-3649.

Soares, A. L. F., van Geemen, D., van den Bogaerdt, A. J., Oomens, C. W. J., Bouten, C. V. C., & Baaijens, F. P. T. (2014). Mechanics of the pulmonary valve in the aortic position. *Journal of the Mechanical Behavior of Biomedical Materials*, *29*, 557-567.

Stradins, P., Lacis, R., Ozolanta, I., Purina, B., Ose, V., Feldmane, L., & Kasyanov, V. (2004). Comparison of biomechanical and structural properties between human aortic and pulmonary valve. *European Journal of Cardio-thoracic Surgery*, *26*(3), 634-639.

Sturla, F., Ronzoni, M., Vitali, M., Dimasi, A., Vismara, R., Preston-Maher, G., ... & Redaelli, A. (2016). Impact of different aortic valve calcification patterns on the outcome of transcatheter aortic valve implantation: a finite element study. *Journal of biomechanics*, *49*(12), 2520-2530.

Thubrikar, M., Piepgrass, W. C., Deck, J. D., & Nolan, S. P. (1980). Stresses of natural versus prosthetic aortic valve leaflets in vivo. *The Annals of Thoracic Surgery*, *30*(3), 230-239.

Yutzey, K. E., Demer, L. L., Body, S. C., Huggins, G. S., Towler, D. A., Giachelli, C. M., ... & Aikawa, E. (2014). Calcific aortic valve disease: a consensus summary from the Alliance of Investigators on Calcific Aortic Valve Disease. *Arteriosclerosis, Thrombosis, and Vascular Biology*, *34*(11), 2387-2393.

© 2021 by the authors; licensee Growing Science, Canada. This is an open access article distributed under the terms and conditions of the Creative Commons Attribution (CC-BY) license (http://creativecommons.org/licenses/by/4.0/).